Open Access Full Text Article

ORIGINAL RESEARCH

Kanglaite reverses multidrug resistance of HCC by inducing apoptosis and cell cycle arrest via PI3K/AKT pathway

Chendong Yang[1,*]
Aihua Hou[1,2,*]
Chunfeng Yu[1]
Lingling Dai[1]
Wen Wang[1]
Kangle Zhang[1]
Hongmin Shao[1]
Jinghua Ma[1]
Wenjuan Xu[2]

[1]Yantai Hospital of Traditional Chinese Medicine, [2]Binzhou Medical University, Yantai, China

*These authors contributed equally to this work

Correspondence: Wenjuan Xu
Binzhou Medical University, School of Integrated Traditional Chinese and Western Medicine, 346 Guanhai Road, Laishan District, Yantai City, Shandong Province 264003, China
Tel/fax +86 535 691 3372
Email xwjycd@126.com

Background: Multidrug resistance (MDR) frequently contributes to the failure of chemotherapeutic treatments in patients diagnosed with hepatocellular carcinoma (HCC). Revealing the molecular mechanism of MDR is indispensable for the development of effective chemotherapeutic drugs.

Purpose: Due to the low-toxicity modulators to inhibit MDR, we considered that Kanglaite (KLT) is a potential agent for reversing MDR in HCC.

Materials and Methods: BEL-7402/5-fluorouracil (5-FU) and HepG2/adriamycin (ADM) were analyzed for cell viability, colony formation assay, cell scratch assay, and cell cycle analysis and apoptosis assay by flow cytometry. The expression of PARP, caspase-3, Bax, Bcl-2, CDC25C, Cyclin B1 and phosphorylation of PTEN, PI3K, and AKT in HepG2/ADM cells were detected by western blotting.

Results: The proliferation of drug-resistant cell lines BEL-7402/5-FU and HepG2/ADM pretreated with KLT was significantly inhibited when compared with drug alone. KLT could increase the accumulation of ADM in HepG2/ADM cells. In this study, we found that KLT treatment notably reduced cell viability, induced apoptosis and cell cycle arrest in human HepG2/ADM and BEL-7402/5-FU cells, and effectively reversed the MDR by p-glycoprotein (P-gp) inhibition. Moreover, KLT decreased the phosphorylation of AKT and PI3K in KLT-treated HepG2/ADM cells. These data together implied that KLT might reverse drug resistance in HCC by blocking the PI3K/AKT signaling.

Conclusion: We demonstrated that KLT reversed MDR of human HCC by inducing apoptosis and cell cycle arrest via the PI3K/AKT signaling pathway.

Keywords: kanglaite, multidrug resistance, hepatocellular carcinoma, apoptosis, PI3K/AKT pathway

Introduction

Hepatocellular carcinoma (HCC) is the fifth most frequently diagnosed cancer worldwide.[1] Poor prognosis and rapid progression of HCC are reported in East Asia and sub-Saharan Africa, especially in China.[2,3] Chemotherapy remains the curative option for HCC. However, drug resistance frequently contributes to the failure of chemotherapeutic treatments in patients diagnosed with HCC.[4] Currently, the molecular mechanisms underlying the multidrug resistance (MDR) of cancer cells are not fully understood. Revealing the molecular mechanisms of MDR is indispensable for the development of effective chemotherapeutic drugs.

Studies have found that the elevated activity of a multidrug transporter, p-glycoprotein (P-gp), is frequently enriched in the MDR tumor.[5–7] The activity of PI3K/AKT family

has been implicated in the regulation of cell proliferation, MDR, tumor transformation, and cell apoptosis.[8–10] As is well known, PI3K/AKT pathway causes drug resistance, through which mediated tumor cells escape apoptosis.[11–13] Various natural products have been shown to be excellent and reliable sources for pharmaceutical development and to be a useful and effective approach for MDR therapies, such as Schisandrin B and annonaceous acetogenins.[14,15]

Kanglaite (KLT) injection is an extract of the Coix lacryma-jobi seed whose main active ingredient is a triglyceride containing four types of fatty acids. KLT has already been developed for anti-tumor clinical applications.[16] It is used to treat primary malignant tumors, including in lung cancer, liver cancer, gastric cancer, and breast cancer, because of its anti-proliferation and proapoptotic effects on numerous tumor cell lines in vitro and tumor models in vivo,[17–22] when it is combined with some chemotherapeutic agents.

This abundant evidence suggests that KLT may play both protective and sensitizing roles in cancer treatments, but its potential and underlying mechanism for reversing cancer resistance still require further investigation. Being an efficacious formula in the treatment of HCC patients, we have utilized drug-resistant human cell lines, HepG2/HepG2/adriamycin (ADM) and BEL-7402/5-fluorouracil (5-FU), to investigate the potential reversal of drug resistance of HCC. In this study, we aimed to investigate the potential of KLT in reversing cancer drug resistance and explore its underlying mechanisms of action.

Materials and methods
Cell culture and reagents
Human HCC cells (HepG2 and HepG2/ADM and Bel-7402 cells Bel-7402/5-FU) were incubated in RPMI-1640 medium (Thermo Fisher Scientific, Waltham, MA, USA) and DMEM (Thermo Fisher Scientific), supplemented with 10% (v/v) fetal bovine serum (FBS; Thermo Fisher Scientific) and 1% (v/v) penicillin–streptomycin (Thermo Fisher Scientific) at 37°C in a humidified atmosphere of 5% CO_2. KLT injection was purchased from Zhejiang Kanglaite Pharmaceutical Co., Ltd, (Zhejiang, China). PI3K activator (740 Y-P) was purchased from APEXBIO (Houston, TX, USA). It is a peptide with the sequence RQIKIWFQNRRMKWKKSDGGYM-DMS and a molecular weight of 3,270.72 Da. LY294002 was obtained from Sigma (St Louis, MO, USA). HepG2 and HepG2/ADM cell lines were obtained from American Type Culture Collection (ATCC, Manassas, VA, USA) and Nanjing Keygen Biotech. Co. (Nanjing, China) respectively. Bel-7402 cells and Bel-7402/5-FU cell lines were kindly provided by Dr Zhang of LUYE PHARMA Group Ltd

(Yantai, China). All procedures involving laboratory cells were approved by the institutional review board of Binzhou Medical University.

Measurement of cell viability
Cell viability assays were performed using the Cell Counting Kit-8 (CCK-8; Dojindo Molecular Technologies, Kumamoto, Japan). Cells were seeded with culture medium onto 96-well plates (1×10^5 cells/mL; 100 µL) and incubated at 37°C for 24 h. After adaptation, cells were treated with KLT, ADM, 5-FU, or cisplatin (CDDP), in combination for 24 and 48 h. Then, the culture medium was replaced with fresh medium containing 10 mL of CCK-8 solution. The optical density (OD) at 490 nm was assayed after cell incubation at 37°C for 2 h.

The coefficient of drug interaction (CDI) analysis for evaluating the effects of drug combinations was calculated according to the study by Cao and Zhen[23] using the equation: CDI = AB/(A × B). A or B is the ratio of the single-agent group to the control group and AB is the ratio of the combination groups to the control group. A CDI ≤ or >1 indicates synergy, additivity, or antagonism of the drugs. A CDI <0.7 shows that the drugs are significantly synergistic.

Colony formation assay
Cells were plated in 6-cm dishes (1×10^5 cells/mL) and incubated in RPMI-1640 or DMEM with 10% FBS at 37°C. Two weeks later, the cells were fixed and stained with 0.1% crystal violet. The number of visible colonies was counted manually.

Cell cycle analysis and apoptosis assay by flow cytometry
Cells were treated with KLT for 48 h, and then the cell cycle analyses were performed. In brief, 5×10^4 cells were suspended in 0.5 mL of propidium iodide (PI) solution and incubated for 30 min in the dark according to the manufacturer's instructions. Cell cycle distribution was analyzed by fluorescence-activated cell sorting (FACS) flow cytometry.

Cells were stained with Annexin V-fluorescein isothiocyanate (FITC) apoptosis detection kit (BD Biosciences, San Jose, CA, USA). According to the manufacturer's instructions, the cells were incubated with 5 mL of Annexin V and 5 mL of PI for 15 min at room temperature, and then the stained cells were analyzed on a FACS flow cytometer.

Hoechest 33258 staining
Nuclear fragmentation was visualized by Hoechst 33258 staining of apoptotic nuclei. Cells were seeded at 4×10^5 cells/

well in six-well plates, incubated overnight for adherence, and treated with KLT. Cells were harvested and washed twice with phosphate-buffered saline (PBS), fixed with 4% paraformaldehyde for 10 min, stained with Hoechst 33258 (1 µg/mL) for 30 min in the dark, and examined under fluorescence microscope.

Gene and protein expression analysis

Gene expression was analyzed by reverse transcription polymerase chain reaction (RT-PCR). Total RNA was extracted using TRIZOL reagent (Thermo Fisher Scientific) according to the manufacturer's instructions. The first-strand cDNA synthesis was performed using cDNA synthesis kit (TaKaRa, Dalian, China). Quantitative RT-PCR was performed using the SYBR Green real-time PCR kit (TaKaRa). The fold changes were calculated by the delta–delta Ct method. All experiments were performed in three biological replicates.

Protein expression was analyzed by Western blot. Total protein (50 µg) was separated by sodium dodecyl sulfate polyacrylamide gel electrophoresis. After protein transfer to polyvinylidene fluoride microporous membranes (Bio-Rad Laboratories Inc., Hercules, CA, USA), the membranes were blocked with 5% nonfat dry milk and incubated sequentially with the primary antibodies (anti-poly (ADP-ribose) polymerase [PARP], anti-caspase-3, anti-Bax, anti-Bcl-2, anti-PI3K, anti-p-AKT^{Ser473}, anti-PTEN [1:1,000 dilution; CST, Boston, MA, USA], or anti-P-gp [1:1,000 dilution; Abcom, London, UK]), followed by incubation with the fluorescein-linked anti-mouse (anti-rabbit) IgG (1:1,000) and then incubation with anti-fluorescein alkaline phosphatase-conjugated antibody (1:5,000). The immune complexes were detected using the enhanced chemiluminescence reagent. For quantification, signals were densitometrically normalized to β-actin by Quantity One image analysis software (Bio-Rad, Hercules, CA, USA).

Accumulation of ADM in cells

Cells were seeded at 4×10^5 cells/well in six-well plates and incubated overnight for adherence and treated with ADM. Cells were harvested and washed twice with PBS, fixed with 4% paraformaldehyde for 10 min, and then examined under fluorescence microscope.

Statistical analysis

Each experiment was repeated at least three times. Data are presented as mean ± SD. All data were analyzed using the SPSS statistical package (version 16.0; SPSS Inc., Chicago, IL, USA). Data between two groups were compared using two-sample tests. Mean values of data from more than three

groups were compared using one-way analysis of variance (ANOVA), and multicomparison was performed. $P<0.05$ was considered as statistically significant.

Results
Cytotoxicity and chemotherapeutics sensitivity of KLT

To address the role of KLT on the cell viability and chemotherapeutics sensitivity. HCC cell lines, including HepG2 and HepG2/ADM, were treated with different concentrations of KLT (0–160 µg/mL). As shown in Figure 1A, KLT significantly inhibited the growth both in a dose- and time-dependent manner in HepG2 and HepG2/ADM cells with an IC$_{50}$ value of 48.85 (HepG2) and 148.77 (HepG2/ADM) µg/mL at 48 h. The results also showed that 20 µg/mL KLT was not cytotoxic (inhibition rate, <5%–10%) and 40 µg/mL KLT was weakly cytotoxic (inhibition rate, 10%–15%) for HepG2/ADM cells. Thus, treatment concentrations of 20 and 40 µg/mL KLT were chosen to study the reversal effects on multiple anticancer drugs in HepG2/ADM cells.

The sensitivity assay showed that HepG2/ADM cells were resistant not only to ADM but also to multiple anticancer drugs, including 5-FU and CDDP. Their lethal dose was significantly higher for HepG2/ADM cells than for non-resistant parental cells (Table 1). Furthermore, we investigated the activity of 20 µg/mL KLT effect on drug resistance. The results showed that KLT significantly decreased the chemoresistance and exhibited synergistic effects with ADM in HepG2/ADM cells (Tables 1 and 2 and Figure 1B–D).

The viability of BEL-7402/5-FU cells treated with KLT was determined by the CCK-8 assay. KLT could inhibit the growth of BEL-7402/5-FU cells in a dose-dependent manner in vitro (Figure S1). Compared with Bel-7402 cells, Bel-7402/5-FU cells had obvious chemoresistance. Twenty µg/mL KLT could enhance the cytotoxicity of multiple anticancer drugs and exhibit synergistic effects with 5-FU for Bel-7402/5-FU cells (Tables S1 and S2 and Figure S1).

KLT reverses the MDR by inhibition of MDR-related genes expression

Adriamycin has natural fluorescent color and has spontaneous fluorescence. The intracellular fluorescence intensity which could reflect the accumulation of intracellular ADM was investigated by the inverted fluorescence microscope. As shown in Figure 2A, compared with the untreated group, the intracellular fluorescence intensity of ADM increased progressively in HepG2/ADM cells. The results indicated that KLT could increase the accumulation of ADM in HepG2/ADM cells.
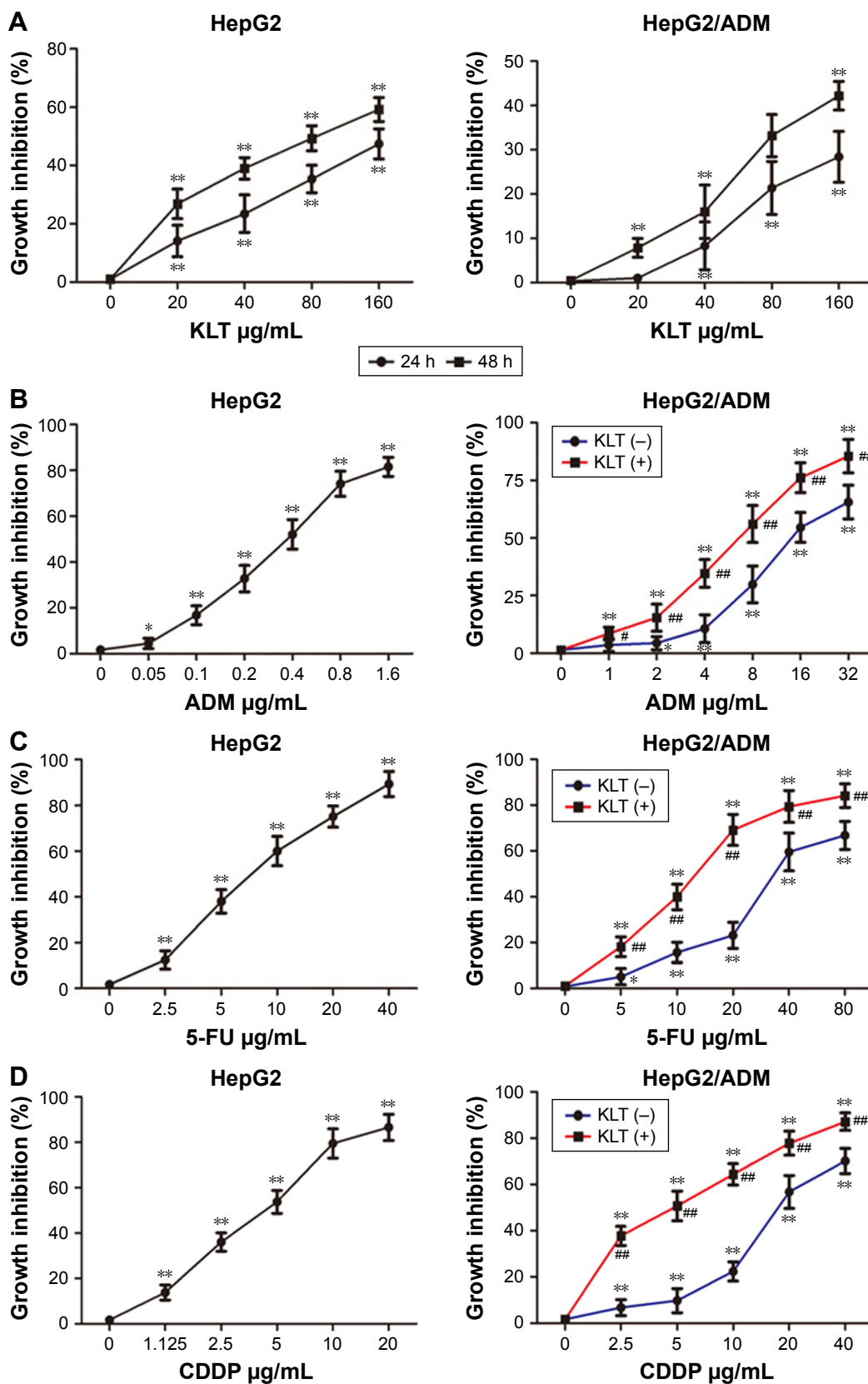
Figure 1 Cytotoxicity and chemotherapeutics sensitivity of KLT.
Notes: (**A**) The percentage of viable cells were measured by the CCK-8 assay at 24 and 48 h relative to no-drug controls and KLT, and concentrations were plotted as a dose–response curve (n=6 per group). HepG2/ADM cells were treated with ADM (**B**), 5-FU (**C**), and CDDP (**D**) for 48 h with or without the pretreatment of KLT (20 μM), and the cell viability was determined by CCK-8 assay. *$P<0.05$; **$P<0.01$ vs control and #$P<0.05$; ##$P<0.01$ vs drug alone (one-way ANOVA, post hoc comparisons, and Tukey's test). Columns represent the mean from three independent experiments, and bars represent SDs.
Abbreviations: ADM, adriamycin; ANOVA, analysis of variance; CCK-8, Cell Counting Kit-8; CDDP, cisplatin; 5-FU, 5-fluorouracil; KLT, Kanglaite.

Table I Comparison of sensitivities to different chemotherapeutic drugs in HepG2 and HepG2/ADM cells

	ADM, IC_{50} (μg/mL)	5-FU, IC_{50} (μg/mL)	CDDP, IC_{50} (μg/mL)
HepG2	0.38	4.36	8.38
HepG2/ADM	14.85	18.66	36.51
HepG2/ADM + KLT	3.35	5.99	15.02
Resistance fold	39.08	4.28	4.36
Reversal fold	4.43	3.11	2.43

Abbreviations: ADM, adriamycin; CDDP, cisplatin; 5-FU, 5-fluorouracil; KLT, Kanglaite.

Members of the ATP-binding cassette subfamily B member 1 (ABCB1)/MDR1 subfamily are involved in MDR. P-gp is the major membrane transporter protein that is involved in efflux activities and leads to MDR.[24] So we wanteds to investigate whether KLT could downregulate the expression of these proteins to restore the intercellular accumulation of ADM. The results of RT-PCR and Western blotting showed that KLT significantly decreased the expression of P-gp in HepG2/ADM and BEL-7402/5-FU cells (Figures 2B and C and S2). These results further confirmed that KLT reversed the MDR by inhibition of P-gp expression.

KLT inhibits colony formation and induces cell cycle arrest in HCC cells

Our results showed that the colony-forming ability of HepG2/ADM cells could be affected by the exposure to KLT (Figure 3A). The treatment of HepG2/ADM and BEL-7402/5-FU cells with KLT for 48 h significantly increased cells in G2/M phase of cell cycle (Figures 3B and S3A). In addition, the KLT enhanced the accumulation of cells in the G2/M phase compared to the single agents.

KLT induces apoptosis in HCC cells

Given the superior synergistic interactions observed with KLT, we investigated the potential effects on cell apoptosis mediated by KLT. Hoechst 33342 staining and Annexin V/PI double staining showed that most of the cell death induced by

Table 2 CDI of the combination of KLT and ADM in HepG2/ADM cells

Concentrations (μg/mL)		HepG2/ADM
KLT	ADM	
20	4	0.790
20	8	0.683
20	16	0.580
20	32	0.435

Abbreviations: ADM, adriamycin; CDI, coefficient of drug interaction; KLT, Kanglaite.

KLT can be classified as apoptosis in both HepG2/ADM and BEL-7402/5-FU cells (Figures 4A and B and S3B). We also observed that the KLT significantly increased early apoptotic cell death. These data revealed an additive mechanism of the KLT inducing cell death via apoptosis.

KLT suppresses expression of PARP, caspase-3, Bax, Bcl-2, CDC25C, and cyclin B1 in HCC cells

Activation of caspases is a biochemical feature of apoptosis. Immunoblotting assessment (Figure 5A and B) showed that the cleavage of PARP and caspase-3 was also increased in HepG2/ADM cells, which were treated with the KLT, in agreement with cell death assays. Western blotting revealed a marked decrease in the expression of Bcl-2 and an increase in the expression of Bax in HepG2/ADM cells treated with KLT compared with control groups. On the basis of the above result, we further detected the protein expression of cell cycle-related proteins. Compared with the control group, the expression of CDC25C and Cyclin B1 was markedly decreased in KLT-treated HepG2/ADM cells (Figure 5A and B).

KLT regulates the PI3K/AKT signaling pathway in HepG2/ADM

It has been reported that the activation of PI3K/AKT signaling pathway followed by AKT phosphorylation plays a role in regulation of cell survival, apoptosis, and drug resistance.[25] To study the mechanisms of KLT on the reversal of MDR, we examined the expression and phosphorylation of PTEN, PI3K, and AKT in HepG2/ADM cells by Western blotting (Figure 6A). The marked phosphorylation of AKT and PI3K was decreased in HepG2/ADM cells treated with KLT. These data together implied that KLT might inhibit AKT with the involvement of PTEN activation and PI3K inhibition.

To further identify the role of AKT in KLT-mediated cell drug resistance, we employed the inhibitor LY294002 or PI3K activator for pretreatment of Hep G2/ADM cells. The results showed that the inactivation of AKT by LY294002 had a large effect on sensitization of HepG2/ADM cells toward cytotoxicity of the combinational treatment with KLT and ADM and strikingly increased apoptosis (Figure 6B and C). Moreover, pretreatment with PI3K activator (50 μg/mL) attenuated KLT and ADM induced apoptosis in HepG2/ADM cells (Figure 6C). In addition, combined treatment of LY294002 and KLT increased the expression of P-gp and CDC25C compared with KLT treatment alone. Pretreatment with PI3K activator strikingly decreased the expression of P-gp and CDC25C compared with KLT treatment alone (Figure 6D). These data together implied that KLT might
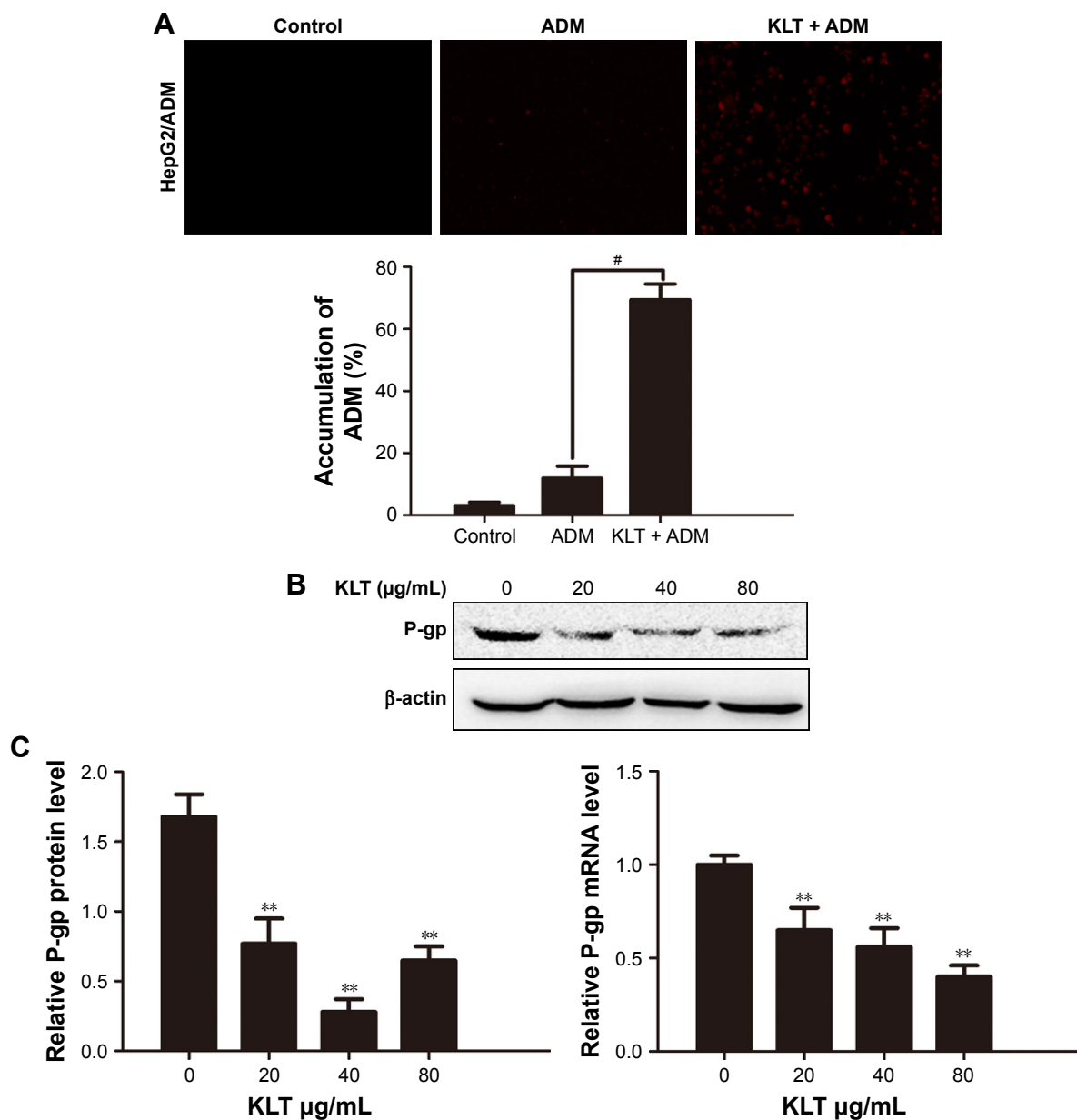
A

Figure 2 KLT reverses the MDR by inhibition of MDR-related genes expression.
Notes: (**A**) The intracellular fluorescence intensity of the accumulation of ADM assessed by the inverted fluorescence microscope. The above assays of ADM accumulation were quantified. (**B**) The expression levels of P-gp were detected by Western blot analysis. Results represent mean values of three experiments (±SD). (**C**) Gene expression analysis of P-gp in HepG2/ADM cells by quantitative real-time PCR. The relative quantification value, fold difference, is expressed as $2^{-\Delta\Delta Ct}$. Data represent three independent experiments. $^{\#}P<0.05$ vs ADM and $^{**}P<0.01$ vs control (one-way ANOVA, post hoc comparisons, and Tukey's test). Columns represent the mean from three independent experiments, and bars represent SDs.
Abbreviations: ADM, adriamycin; ANOVA, analysis of variance; KLT, Kanglaite; MDR, multidrug resistance; PCR, polymerase chain reaction; P-gp, p-glycoprotein.

regulate the PI3K/AKT pathway with the involvement of tumor cell drug resistance by inducing apoptosis and cell cycle arrest.

Discussion

HCC is a hypervascular tumor with the characteristic of high levels of neovascularization and angiogenesis.[26] Disappointing results of numerous trials testing the efficacy of various drugs indicate that HCC has low sensitivity to

chemotherapy that is in great part caused by MDR.[27] Until now, many attempts have been made to restore the chemosensitivity of chemotherapeutic agents. Delivery of miR-375 and doxorubicin hydrochloride by lipid-coated hollow mesoporous silica nanoparticles could overcome multiple drug resistance in hepatocellular carcinoma.[28] Ubiquitin-specific protease 22 (USP22) mediates the MDR of HCC via the SIRT1/AKT/MRP1 signaling pathway.[29] Overexpression of protein phosphatase 1γ (PP1γ) is associated with enhanced
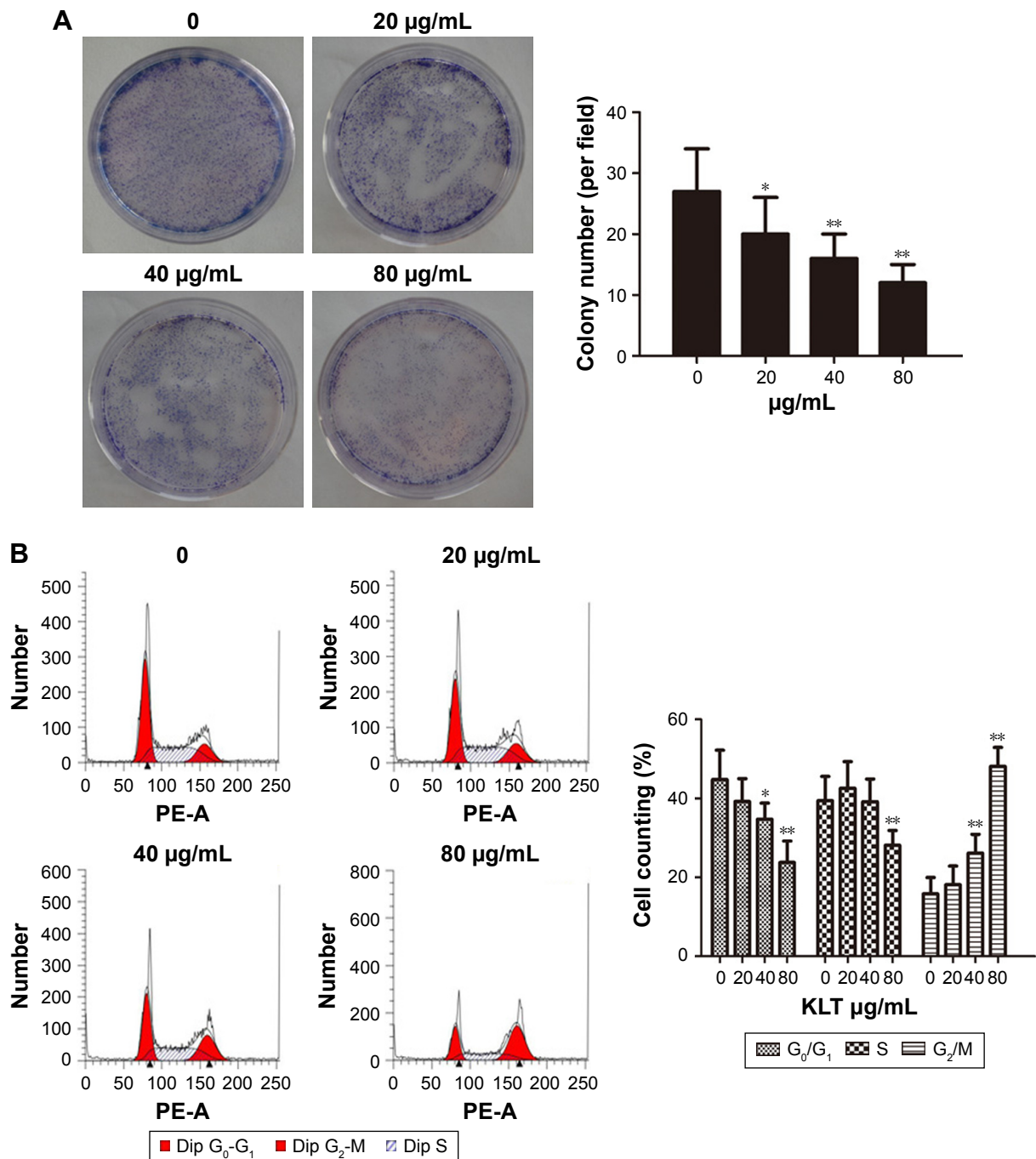
A

B

Figure 3 KLT inhibits colony formation and induces cell cycle arrest in hepatocellular carcinoma cells.
Notes: (**A**) Representative images were captured from HepG2/ADM cells incubated with KLT for 48 h and subjected to cell colony-formation assays. These assays were quantified. (**B**) Cell cycle distribution of HepG2/ADM cells was determined 48 h after treatment with KLT (n=3). These assays were quantified. *$P<0.05$ and **$P<0.01$ vs control (one-way ANOVA, post hoc comparisons, Tukey's test). Columns represent the mean from three independent experiments, and bars represent SDs.
Abbreviations: ADM, adriamycin; ANOVA, analysis of variance; Dip, diploid; KLT, Kanglaite; MDR, multidrug resistance; P-gp, p-glycoprotein.

cell proliferation and poor prognosis in HCC.[30] According to reports, the mechanism of resistance to chemotherapy may be associated with the classical drug-resistant pathway, which is mediated by P-gp, and the inhibition on cell apoptosis, which are the two most investigated mechanisms in research for MDR of tumors.

Due to the low-toxicity modulators to inhibit MDR, we considered that KLT is a potential agent for reversing multidrug resistance in HCC. KLT has shown anti-tumor effects in various types of tumors, including HCC. Moreover, it was shown that KLT has anti-cancer activities against HCC, but a high concentration was needed. Our results showed that
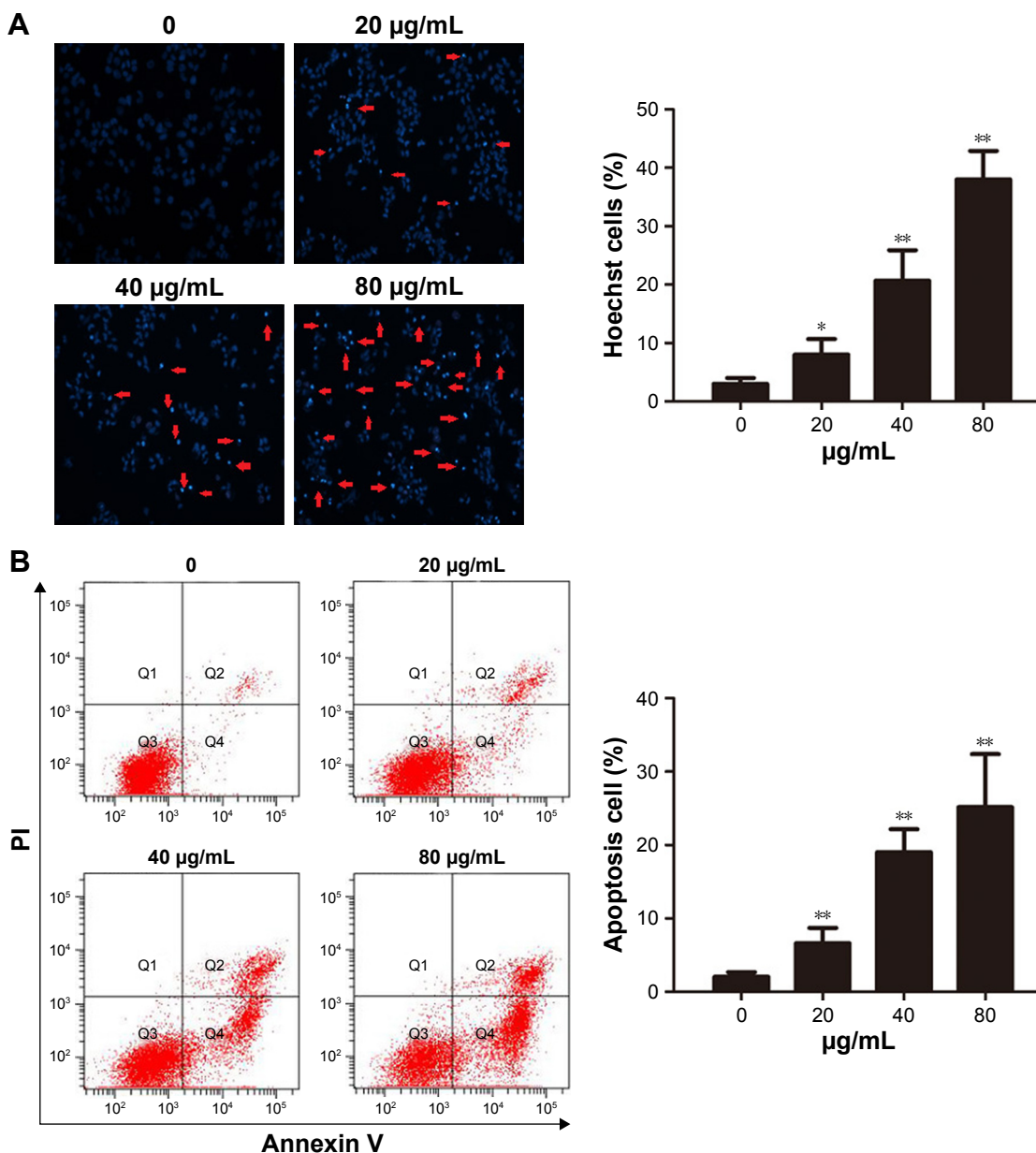
Figure 4 KLT induces apoptosis in hepatocellular carcinoma cells.
Notes: (**A**) Cells were stained with Hoechst 33342 (5 μg/mL) and subjected to analysis of apoptosis population (n=3). (**B**) PE-Annexin V staining of phosphatidylserine exposed on the cell surface was measured by flow cytometric analysis (n=3). Data derived from three separate experiments are presented as the mean ± SD. *$P<0.05$ and **$P<0.01$ vs control (one-way ANOVA, post hoc comparisons, and Tukey's test). Columns represent the mean from three independent experiments, and bars represent SDs.
Abbreviations: ANOVA, analysis of variance; KLT, Kanglaite; PI, propidium iodide.

the proliferation of drug-resistant cell line BEL-7402/5-FU and HepG2/ADM was significantly inhibited after cells were pretreated with KLT, compared with drug alone. KLT could increase the accumulation of ADM in HepG2/ADM cells and significantly decrease the expression of P-gp in HepG2/ADM and BEL-7402/5-FU cells. These results further confirmed that KLT reversed the MDR by the inhibition of P-gp expression.

However, the mechanism by which KLT enhances chemotherapeutics sensitivity against HCC remains unclear.

This study demonstrated that the KLT exhibited more potent anti-tumor effects in terms of cytotoxicity, colony formation, cell cycle arrest, and apoptotic induction in human HepG2/ADM and BEL-7402/5-FU cells. Western blot revealed a marked decrease of cell cycle-related molecules, CDC25C and Cyclin B1, and an increase of cleaved caspase-3, cleaved PARP, and Bax in KLT-treated HepG2/ADM cells. These results implied that KLT induced the apoptosis and cell cycle arrest of HCC cells to reverse drug resistance.
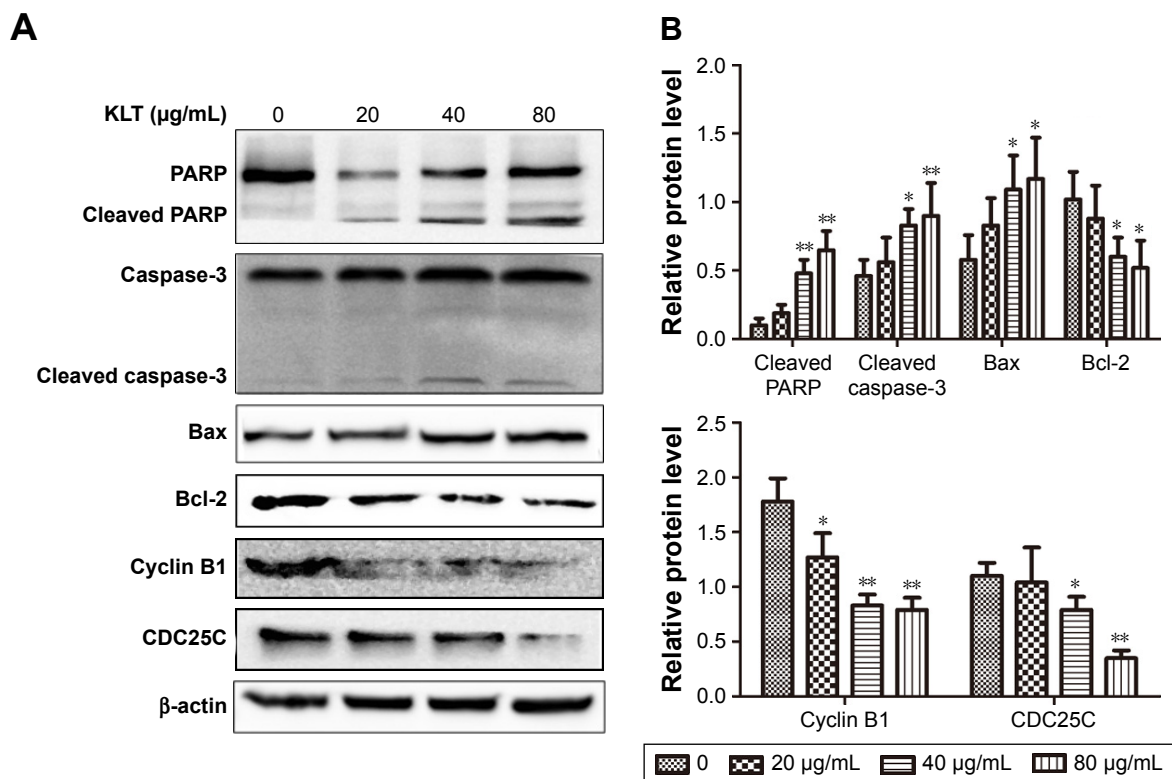
A

B

Figure 5 KLT suppresses the expression of PARP, caspase-3, Bax, Bcl-2, CDC25C, and cyclin B1 in hepatocellular carcinoma cells.

Notes: (**A**) Total cell lysates were prepared for Western blot analysis of the apoptosis regulatory proteins and cell cycle-related proteins (n=3). (**B**) The densitometric analysis bar diagram of the results. Columns represent the mean from three independent experiments and bars represent SDs. *$P<0.05$ and **$P<0.01$ vs control (one-way ANOVA, post hoc comparisons, and Tukey's test). Columns represent the mean from three independent experiments, and bars represent SDs.

Abbreviations: ANOVA, analysis of variance; KLT, Kanglaite; PARP, poly (ADP-ribose) polymerase.

Other results of Western blot analysis showed that KLT decreased phosphorylation of AKT and PI3K in KLT-treated HepG2/ADM cells. LY294002 and PI3K activator affected the apoptosis induced by KLT and ADM in HepG2/ADM cells. In addition, combined treatment of LY294002 and KLT increased the expression of P-gp and CDC25C, which was strikingly decreased by the pretreatment with PI3K activator compared with KLT treatment alone. These data together implied that KLT might regulate the PI3K/AKT with

the involvement of tumor cell drug resistance. The PI3K/AKT signaling pathway controls the expression and function of many proteins that are necessary for tumor cell drug resistance to escape apoptosis.[31] Some evidence indicates that the PI3K/AKT signaling pathway enhances drug efflux by ABC transporters, maintaining the drug resistance of tumor cells. MEK inhibitors induce AKT activation and drug resistance by suppressing negative feedback ERK-mediated HER2 phosphorylation at Thr701.[32] Integrin β1-mediated
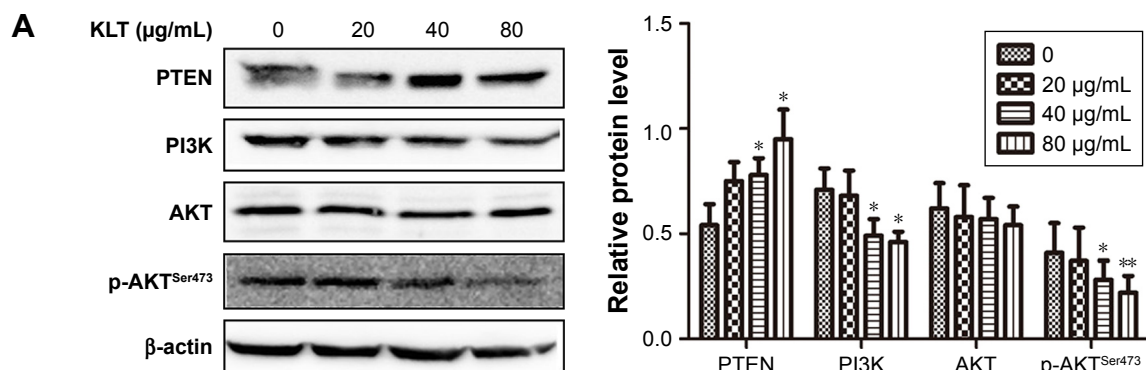
A

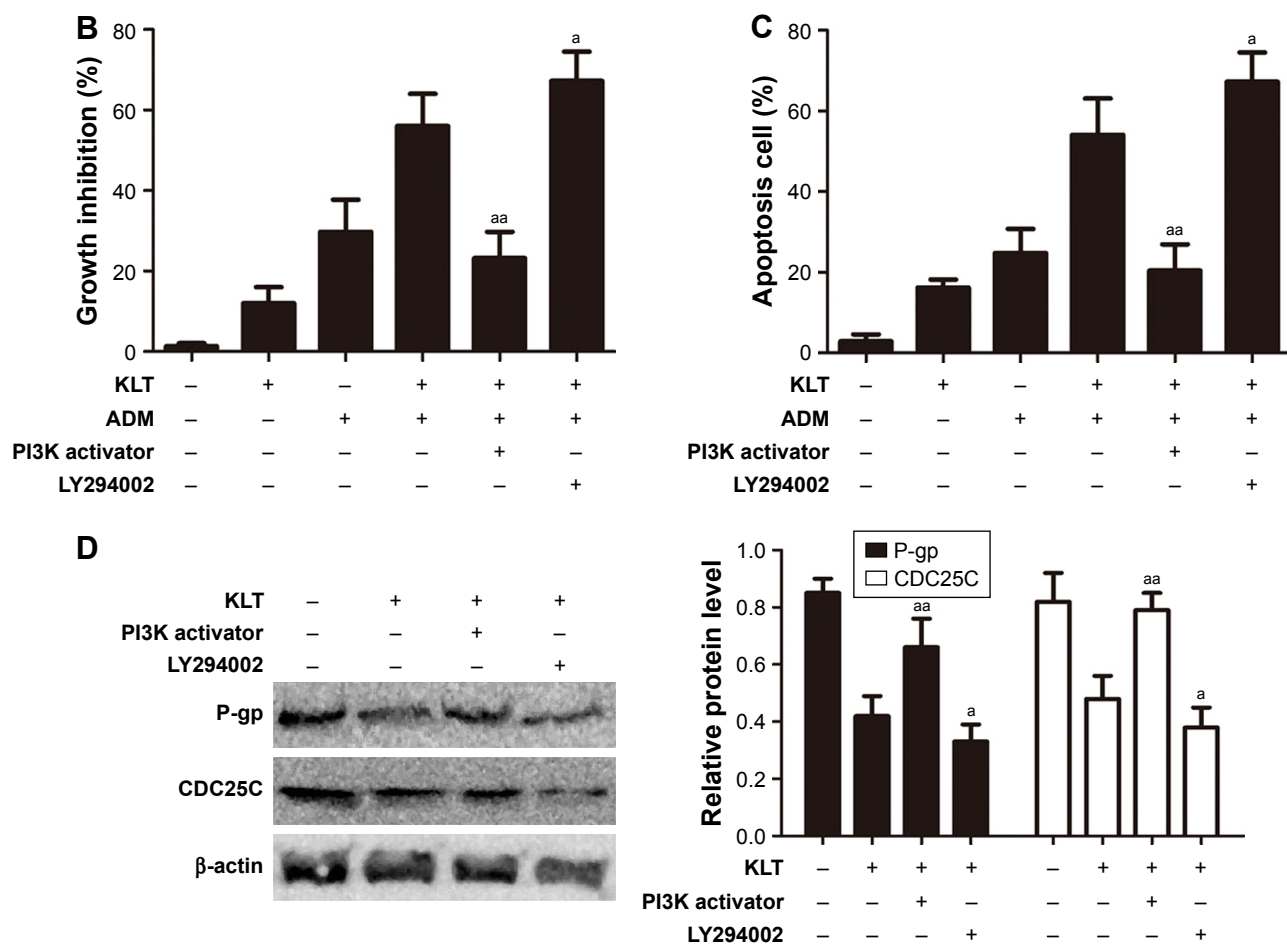
Figure 6 (*Continued*)

Figure 6 KLT regulates the PI3K/AKT signaling pathway in HepG2/ADM cells.
Notes: (**A**) Total cell lysates were prepared for Western blot analysis of the PI3K/AKT signaling pathway proteins (n=3). The densitometric analysis bar diagram of the results is shown. HepG2/ADM cells were treated with KLT and ADM in the absence or presence of LY294002 (4 μM) and PI3K activator (50 μg/mL). Cell viability was measured by MTT assay (**B**), and the proportion of Annexin V-positive cells was analyzed by flow cytometry (**C**). (**D**) Effect of LY294002 and PI3K activator on MDR and cell cycle arrest by immunoblotting with P-gp and CDC25C. Columns represent the mean from three independent experiments, and bars represent SDs. *$P<0.05$ and **$P<0.01$ vs control, ª$P<0.05$ and ªª$P<0.01$ vs KLT + ADM or KLT (one-way ANOVA, post hoc comparisons, and Tukey's test).
Abbreviations: ADM, adriamycin; ANOVA, analysis of variance; KLT, Kanglaite; MDR, multidrug resistance; MTT, (3-(4,5-dimethylthiazol-2-yl)-2,5-diphenyltetrazolium bromide) tetrazolium; P-gp, p-glycoprotein.

acquired gefitinib resistance in non-small-cell lung cancer cells occurs via the phosphoinositide 3-kinase-dependent pathway.[33] We demonstrated that KLT reversed MDR of human HCC by inducing apoptosis and cell cycle arrest via the PI3K/AKT signaling pathway.

Conclusion

These data demonstrated that KLT treatment notably reduced cell viability, induced apoptosis and cell cycle arrest in human HepG2/ADM and BEL-7402/5-FU cells, and effectively reversed the MDR by inhibiting P-gp expression. The decrease of PI3K/AKT activation was associated with the KLT administration. Overall, these findings have revealed the molecular mechanisms of KLT treatment with HCC, which provides a basis and warrants future study to investigate the combination therapy for the treatment of drug-resistant

tumors with targeted therapy. Further studies are needed to define the effects of the combined treatment with in vivo models of MDR cancer and their underlying mechanism in regulating carcinogenesis.

Data availability

The data sets generated and analyzed in this study are available from the corresponding author on reasonable request.

Acknowledgments

Disclosure

The authors declare no conflict of interest.

References

1. Torre LA, Bray F, Siegel RL, Ferlay J, Lortet-Tieulent J, Jemal A. Global cancer statistics, 2012. *CA Cancer J Clin*. 2015;65(2):87–108.
2. Ma L, Chua MS, Andrisani O, So S. Epigenetics in hepatocellular carcinoma: an update and future therapy perspectives. *World J Gastroenterol*. 2014;20(2):333–345.
3. Ruan J, Zheng H, Rong X, et al. Overexpression of cathepsin B in hepatocellular carcinomas predicts poor prognosis of HCC patients. *Mol Cancer*. 2016;15:17.
4. Gatenby RA, Smallbone K, Maini PK, et al. Cellular adaptations to hypoxia and acidosis during somatic evolution of breast cancer. *Br J Cancer*. 2007;97(5):646–653.
5. Lotz C, Kelleher DK, Gassner B, Gekle M, Vaupel P, Thews O. Role of the tumor microenvironment in the activity and expression of the p-glycoprotein in human colon carcinoma cells. *Oncol Rep*. 2007; 17(1):239–244.
6. Chen X, Zhang M, Liu LX. The overexpression of multidrug resistance-associated proteins and gankyrin contribute to arsenic trioxide resistance in liver and gastric cancer cells. *Oncol Rep*. 2009;22(1):73–80.
7. Xiang QF, Zhang DM, Wang JN, et al. Cabozantinib reverses multidrug resistance of human hepatoma HepG2/adr cells by modulating the function of P-glycoprotein. *Liver Int*. 2014;35(3):1010–1023.
8. Wang R, Zhang Q, Peng X, et al. Stellettin B induces G1 arrest, apoptosis and autophagy in human non-small cell lung cancer A549 cells via blocking PI3K/Akt/mTOR pathway. *Sci Rep*. 2016;6:27071.
9. Abdul-Ghani R, Serra V, Gyorffy B, et al. The PI3K inhibitor LY294002 blocks drug export from resistant colon carcinoma cells overexpressing MRP1. *Oncogene*. 2006;25(12):1743–1752.
10. Barancík M, Boháčová V, Sedlák J, Sulová Z, Breier A. LY294,002, a specific inhibitor of PI3K/Akt kinase pathway, antagonizes P-glycoprotein-mediated multidrug resistance. *Eur J Pharm Sci*. 2006;29(5):426–434.
11. Hong SW, Jung KH, Lee HS, et al. SB365 inhibits angiogenesis and induces apoptosis of hepatocellular carcinoma through modulation of PI3K/Akt/mTOR signaling pathway. *Cancer Sci*. 2012; 103(11):1929–1937.
12. Tazzari PL, Cappellini A, Ricci F, et al. Multidrug resistance-associated protein 1 expression is under the control of the phosphoinositide 3 kinase/Akt signal transduction network in human acute myelogenous leukemia blasts. *Leukemia*. 2007;21(3):427–438.
13. Liang J, Ge F, Guo C, et al. Inhibition of PI3K/Akt partially leads to the inhibition of PrP(C)-induced drug resistance in gastric cancer cells. *FEBS J*. 2009;276(3):685–694.
14. Qian JQ, Sun P, Pan ZY, Fang ZZ. Annonaceous acetogenins reverses drug resistance of human hepatocellular carcinoma BEL-7402/5-FU and HepG2/ADM cell lines. *Int J Clin Exp Pathol*. 2015;8(9):11934–11944.
15. Wang S, Wang A, Shao M, Lin L, Li P, Wang Y. Schisandrin B reverses doxorubicin resistance through inhibiting P-glycoprotein and promoting proteasome-mediated degradation of survivin. *Sci Rep*. 2017; 7(1):8419.
16. Ye L, Yan L, Xing T, Fu D. Formulation, preparation and evaluation of an intravenous emulsion containing *Brucea javanica* oil and *Coix* seed oil for anti-tumor application. *Biol Pharm Bull*. 2008;31(4):673–680.
17. Qu D, Liu M, Huang M, et al. Octanoyl galactose ester-modified microemulsion system self-assembled by *Coix* seed components to enhance tumor targeting and hepatoma therapy. *Int J Nanomedicine*. 2017;12:2045–2059.
18. Lu Y, Li C, Dong Q. Chinese herb related molecules of cancer-cell-apoptosis: a minireview of progress between Kanglaite injection and related genes. *J Exp Clin Cancer Res*. 2008;27:31–35.
19. Fu F, Wan Y, Mulati, Wu T. Kanglaite injection combined with hepatic arterial intervention for unresectable hepatocellular carcinoma: a meta-analysis. *J Cancer Res Ther*. 2014;10(suppl 1):38–41.
20. Wang J, Sun X, Shen W. Research on apoptosis of cancer cell and expression of p53, bcl-2 protein Induced by KLT Injection. *Chin J Clin Oncol*. 1999;26:439–442.
21. Wang Y, Zhang C, Zhang S, et al. Kanglaite sensitizes colorectal cancer cells to Taxol via NF-κB inhibition and connexin 43 upregulation. *Sci Rep*. 2017;7:1280–1289.
22. Qu D, He J, Liu C, Zhou J, Chen Y. Triterpene-loaded microemulsion using *Coix lacryma-jobi* seed extract as oil phase for enhanced antitumor efficacy: preparation and in vivo evaluation. *Int J Nanomedicine*. 2014;9:109–119.
23. Cao SS, Zhen YS. Potentiation of antimetabolite antitumor activity in vivo by dipyridamole and amphotericin B. *Cancer Chemother Pharmacol*. 1989;24(3):181–186.
24. Cheon JH, Kim KS, Yadav DK, Kim M, Kim HS, Yoon S. The JAK2 inhibitors CEP-33779 and NVP-BSK805 have high P-gp inhibitory activity and sensitize drug-resistant cancer cells to vincristine. *Biochem Biophys Res Commun*. 2017;490(4):1176–1182.
25. Chen H, Li H, Chen Q. INPP4B reverses docetaxel resistance and epithelial-to-mesenchymal transition via the PI3K/Akt signaling pathway in prostate cancer. *Biochem Biophys Res Commun*. 2016;477(3): 467–472.
26. Geis T, Döring C, Popp R, et al. HIF-2alpha-dependent PAI-1 induction contributes to angiogenesis in hepatocellular carcinoma. *Exp Cell Res*. 2015;331(1):46–57.
27. Galun D, Srdic-Rajic T, Bogdanovic A, Loncar Z, Zuvela M. Targeted therapy and personalized medicine in hepatocellular carcinoma: drug resistance, mechanisms, and treatment strategies. *J Hepatocell Carcinoma*. 2017;4:93–103.
28. Xue H, Yu Z, Liu Y, et al. Delivery of miR-375 and doxorubicin hydrochloride by lipid-coated hollow mesoporous silica nanoparticles to overcome multiple drug resistance in hepatocellular carcinoma. *Int J Nanomedicine*. 2017;12:5271–5287.
29. Ling S, Li J, Shan Q, et al. USP22 mediates the multidrug resistance of hepatocellular carcinoma via the SIRT1/AKT/MRP1 signaling pathway. *Mol Oncol*. 2017;11(6):682–695.
30. Li C, Wu M, Zong G, et al. Overexpression of protein phosphatase 1γ (PP1γ) is associated with enhanced cell proliferation and poor prognosis in hepatocellular carcinoma. *Dig Dis Sci*. 2017;62(1):133–142.
31. Zhou B, Sun C, Li N, et al. Cisplatin-induced CCL5 secretion from CAFs promotes cisplatin-resistance in ovarian cancer via regulation of the STAT3 and PI3K/Akt signaling pathways. *Int J Oncol*. 2016; 48(5):2087–2097.
32. Chen CH, Hsia TC, Yeh MH, et al. MEK inhibitors induce Akt activation and drug resistance by suppressing negative feedback ERK-mediated HER2 phosphorylation at Thr701. *Mol Oncol*. 2017;11(9): 1273–1287.
33. Deng QF, Su BO, Zhao YM, Tang L, Zhang J, Zhou CC. Integrin β1-mediated acquired gefitinib resistance in non-small cell lung cancer cells occurs via the phosphoinositide 3-kinase-dependent pathway. *Oncol Lett*. 2016;11(1):535–542.
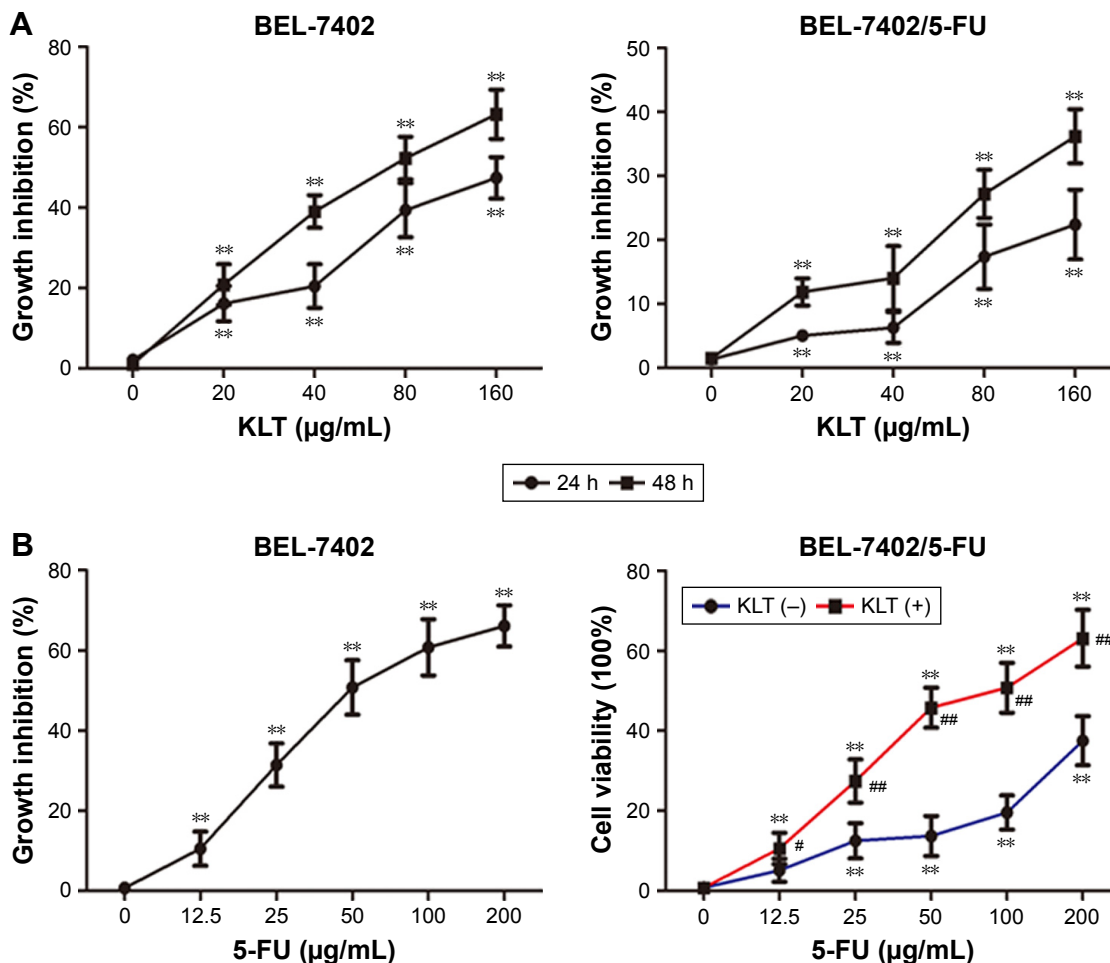
Supplementary materials

Figure S1 Cytotoxicity and chemotherapeutics sensitivity of KLT in BEL-7402/5-FU cells.
Notes: (**A**) The percentage of viable cells was measured by the CCK-8 assay at 24 and 48 h relative to no-drug controls and KLT and concentrations were plotted as a dose response curve (n=6 per group). (**B**) BEL-7402/5-FU cells were treated with , 5-FU for 48 h with or without the pretreatment of KLT (20 μM) and the cell viability was determined by CCK-8 assay. **$P < 0.01$, vs. control, #$P < 0.05$; ##$P < 0.01$ vs. drug alone. One-way ANOVA, post hoc comparisons, Tukey's test. Columns, means; error bars, SDs.
Abbreviations: 5-FU, 5-fluorouracil; ANOVA, analysis of variance; CCK-8, Cell Counting Kit-8; KLT, Kanglaite.

Table S1 Comparison of sensitivities to 5-FU in BEL-7402 and BEL-7402/5-FU cells

	5-FU (IC$_{50}$)
BEL-7402	4.02
BEL-7402/5-FU	10.58
BEL-7402/5-FU + KLT	4.70
Resistance fold	2.63
Reversal fold	2.25

Abbreviations: 5-FU, 5-fluorouracil; IC$_{50}$, half maximal inhibitory concentration; KLT, Kanglaite.

Table S2 CDI of the combination of KLT and 5-FU in BEL-7402/5-FU cells

Concentrations (μg/mL)		HepG2/ADM
KLT	**ADM**	
20	25	0.825
20	50	0.600
20	100	0.513
20	200	0.572

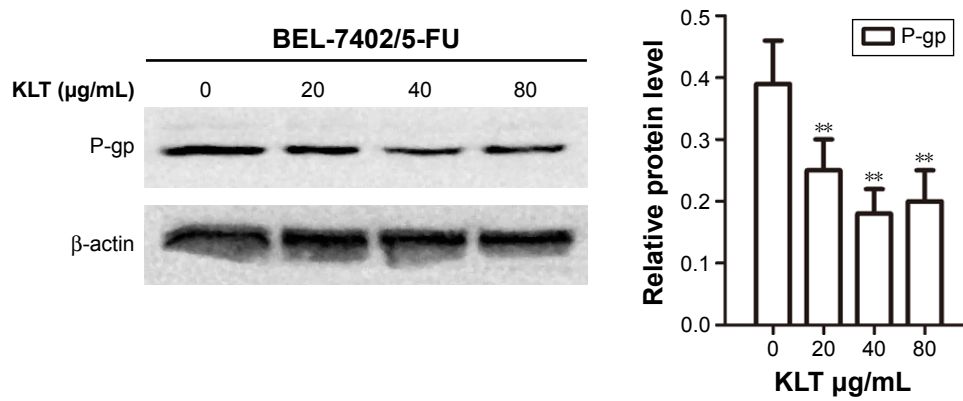**Abbreviations:** CDI, coefficient of drug interaction; 5-FU, 5-fluorouracil; KLT, Kanglaite.

Figure S2 KLT reversed the MDR by inhibition of MDR-related gene expression in BEL-7402/5-FU cells.
Notes: **$P<0.01$, vs. control. One-way ANOVA, post hoc comparisons, Tukey's test. Columns, means; error bars, SDs.
Abbreviations: 5-FU, 5-fluorouracil; KLT, Kanglaite; MDR, multidrug resistance; P-gp, p-glycoprotein.
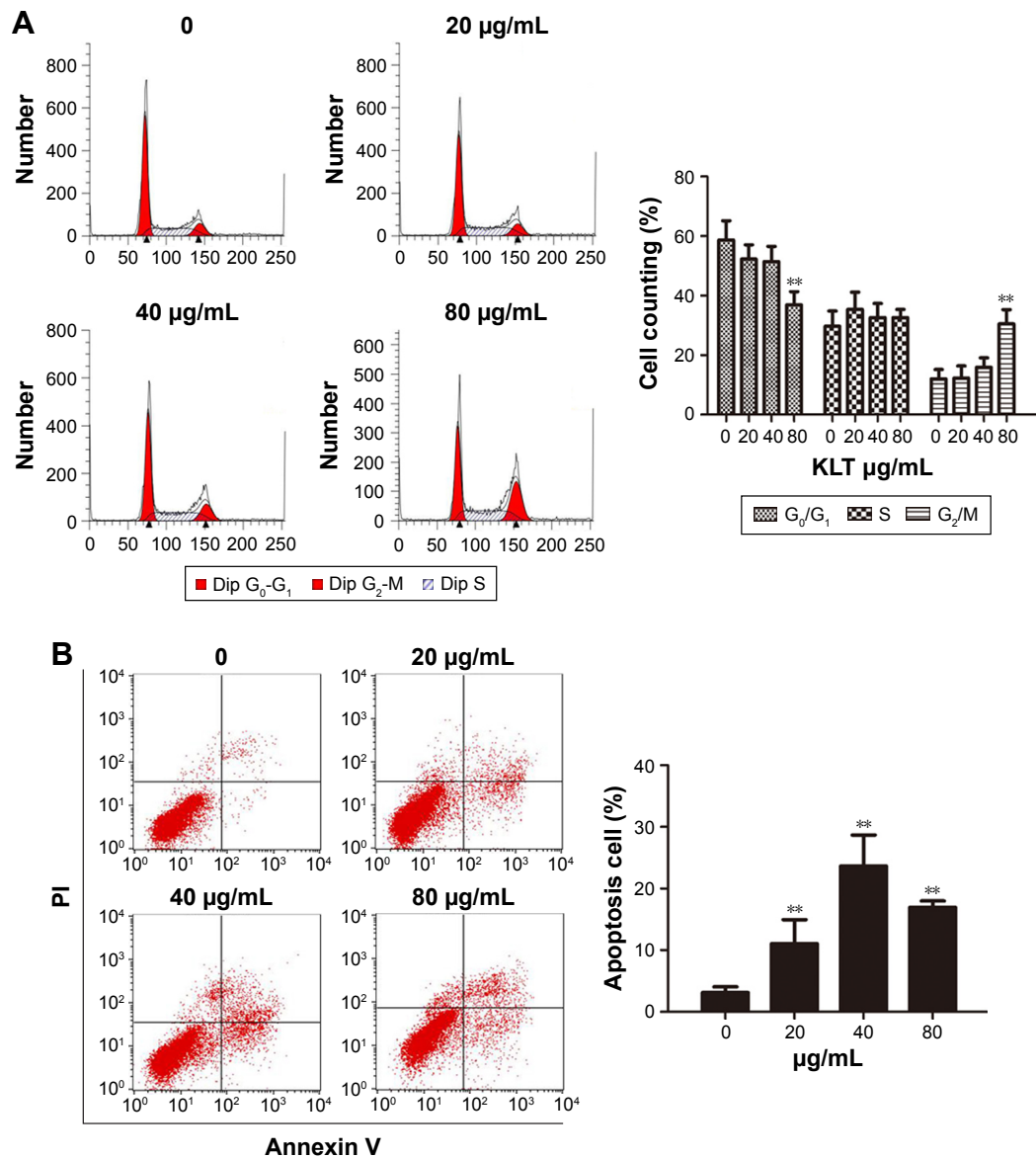

Figure S3 KLT induces cell cycle arrest and apoptosis in BEL-7402/5-FU cells.
Notes: (**A**) Cell cycle distribution of BEL-7402/5-FU cells was determined 48 h after treatment with KLT (n=3). The above assays were quantified. (**B**) PE-Annexin V staining of phosphatidylserine exposed on the cell surface was measured by flow cytometric analysis (n=3). Data derived from three separate experiments are presented as the means ± SD. **$P<0.01$, vs. control, One-way ANOVA, post hoc comparisons, Tukey's test. Columns, means; error bars, SDs.
Abbreviations: 5-FU, 5-fluorouracil; Dip, diploid; KLT, Kanglaite; MDR, multidrug resistance; P-gp, p-glycoprotein; PI, propidium iodide.